JOURNAL OF APPLIED ELECTROCHEMISTRY 22 (1992) 195-199

Properties of electrochemically synthesized polymer electrodes

Part VIII: Kinetics of polypyrrole in polymer electrolyte cells

C. CASAGRANDE, S. PANERO, P. PROSPERI, B. SCROSATI*

Dipartimento di Chimica, Università di Roma 'La Sapienza', 00185, Rome, Italy

Received 9 October 1991; revised 6 June 1991

Results obtained by cyclic voltammetry and frequency response analysis show that the electrochemical behaviour of solid state cells based on the combination of polymer electrolytes and polymer electrodes is crucially affected by the morphology of the electrode interfaces. Fast kinetics and good interfacial contacts can be obtained using composite electrodes electrosynthesized from solutions containing a polymer electrolyte and large surfactant anions.

1. Introduction

Electrochemically synthesized polypyrrole (pPy) is presently considered as one of the most promising polymer electrode materials for the development of advanced electrochemical devices [1, 2]. In this respect, particular interest has recently been devoted to the use of pPy as polymer electrode in solid-state cells using electrolytes based on complexes of poly(ethylene oxide) PEO with lithium salts.

Various authors [3-7] have investigated the properties of this type of cell and the results agree in showing that the cell performance is strongly influenced by the kinetics of the doping-undoping (redox) process of the polymer electrode. Therefore, it seemed of interest to investigate in detail the electrochemical response of pPy film electrodes in solid-state cells using as typical polymer electrolyte the $(PEO)_{20}$ $LiClO_4$ complex.

In this respect, the behaviour of various types of interfaces obtained with pPy electrodes synthesized under different conditions has been examined. The electrochemical study was performed at 70° C (to assure low resistance to the polymer electrolyte cells), using cycling voltammetry (CV) and frequency response analysis (FRA) as testing techniques.

2. Experimental details

Monomer pyrrole (Fluka pure commercial product) was further purified by distillation under vacuum and the final product was stored at low temperature (around 0° C). Polypyrrole film samples were galvanostatically deposited onto stainless steel (SS) substrates from various types of solution having different nature and composition, namely:

(a) acetonitrile (AN) solution containing monomer pyrrole (Py 0.2 M) and $LiClO_4$ (0.5 M) as supporting electrolyte. AN (Fluka pure commercial product) was further purified by distillation under a nitrogen stream. $LiClO_4$ (Fluka pure product) was further purified by melting under vacuum and keeping it at 250° C for about 20 min.

(b) AN solution containing Py (0.2 M), $(PEO)_{20}$-$LiClO_4$. Poly(ethylene oxide), PEO, was a BDH product having a molecular weight MW = 4 000 000.

(c) AN solution containing Py (0.2 M) and sodium dodecylsulphate, $C_{12}H_{25}O_4SNa$ (SDS, satured solution) as supporting electrolyte. SDS (Fluka pure commercial product) further purified by recrystallization from methanol.

(d) AN solution of Py (0.2 M), SDS-PEO (satured solution).

The morphology of the electrodeposited pPy films was varied by monitoring the current density, while the thickness was controlled by varying the total charge passed in the electrosynthesis cell. Table 1 describes the type of pPy samples used in this work, in terms of the nature of the electrosynthesis solution, the current density, the charge passed and the thickness of the final samples.

After electrodeposition, the pPy samples were thoroughly washed with pure solvent (to eliminate traces of residual monomer) and dried (to eliminate traces of residual solvent). The samples were then moved to the electrochemical testing cells. These cells, consisting in a dried pPy sample working electrode, a layer of the $(PEO)_{20}LiClO_4$ polymer electrolyte, and a counter electrode, were housed in a Teflon container. The nature of the counter electrode varied according to the type of measurement, being either a lithium disc (CV and FRA) or the same pPy film (FRA). The cell

---

* Author to whom all correspondence should be addressed

Table 1. Conditions of synthesis of pPy samples

Synthesis solution	Synthesis current/ mA cm^{-2}	Charge/ mC cm^{-2}	Film thickness/ μm
(a) $LiClO_4$-AN 0.5 M	7	196	0.8
(b) AN-$(PEO)_{20}LiClO_4$	1	360	1.5
(c) SDS-AN saturated solution	1 7	360 196	1.5 0.8
(d) SDS-AN-PEO saturated solution	1	360	1.5

was kept in an oven (Bucki Mod. TO/51) for temperature control.

The $(PEO)_{20}LiClO_4$ polymer electrolyte was prepared by a standard casting procedure which included the dissolution of the components (i.e. PEO and $LiClO_4$ in the desired composition ratio) in acetonitrile, the homogenization of the solution in flat Teflon container and followed by the slow evaporation of the solvent in order to cast $(PEO)_{20}LiClO_4$ films of average thicknesses between 50 and 100 μm. The cell assembly and polymer electrolyte preparation were both carried out in argon-filled dry boxes, having a moisture content less than 10 p.p.m.

Cyclic voltammetry (CV) curves were obtained using an AMEL mod. 551 potentiostat coupled with an AMEL mod. 567 function generator and registered with an X-Y recorder. Frequency response analysis (FRA) was carried out using a Solartron mod. 1250 analyser coupled with a Solartron mod. 1286 electrochemical interface. The results were examined and analysed using a modified version of the Boukamp fitting program [8].

3. Results and discussion

3.1. *Cyclic voltammetry*

Figure 1 illustrates the cyclic voltammograms for pPy samples (a) and (b) (see Table 1 for identification), obtained at 70° C in a solid-state cell using $(PEO)_{20}LiClO_4$ as polymer electrolyte and lithium as counter electrode, i.e. a cell of the following composition:

$$Li \mid (PEO)_{20}LiClO_4 \mid pPy(SS) \qquad (1)$$

The relevant voltammetric data are summarized in Table 2.

First, we observe that the voltammogram of sample (a), i.e. the sample electrodeposited from a $LiClO_4$-AN solution, shows a very poor peak definition and a large peak separation. Furthermore, the cycling charge is very modest, i.e. confined to 0.15% maximum doping level. It is worth noting that the doping level, y, is defined as the percentage of moles of the doping counteranions (e.g. ClO_4^-) over the moles of the monomeric pyrrolic unit [24].

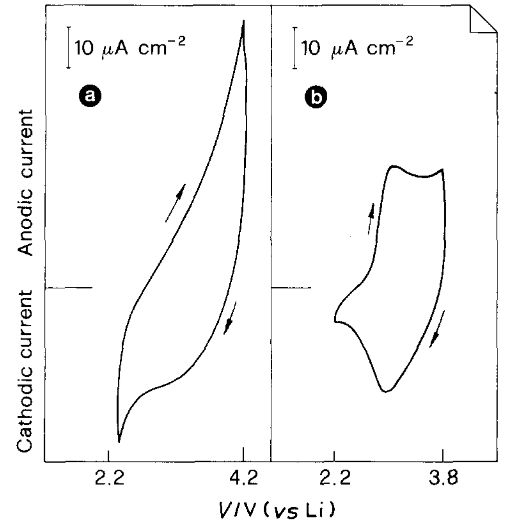

Fig. 1. Cyclic voltammetry of polypyrrole in a lithium cell having a $(PEO)_{20}LiClO_4$ polymer electrolyte. The curves are related to samples (a) and (b) and are obtained at 70° C and at 50 mV s − 1. For identification of samples see Table 1.

The results of Table 2 clearly show that the electrochemical reversibility of this type of sample (a) is poor and that the kinetics of the related electrochemical reaction are slow.

As is well known [1], this electrochemical reaction involves the oxidation of the polymer and a charge compensation exerted by injection of counterions from the electrolyte into the polymer itself. This type of mechanism implies the diffusion of the ions, both through the solid polymer electrolyte and through the solid, polymer electrode [1]. As generally observed in the case of a diffusion-controlled electrochemical process [3], the morphology of the interface plays a key role in controlling the overall kinetics and thus the realization of a smooth solid/solid interfacial contact is crucial in assuring fast and reversible behaviour of the pPy electrode in the solid-state polymer electrolyte cell.

In view of this, it is not surprising that interfaces merely formed by contacting the pPy film electrode with a layer of the polymer electrolyte (likely to have a high degree of nonsuniformity) show very poor kinetics, as observed in the case of Fig. 1a.

The morphological conditions of the interface can be substantially improved by synthesizing pPy film

Table 2. Voltammetric data for pPy film electrodes synthesized under various conditions. Temperature: 70° C, scan rate: 50 mV s^{-1}

Synthesis solution	Doping Level y/%	Peak separation ΔE_p/mV	Redox potential E_0/V vs Li^+
(a) $LiClO_4$-AN	0.15	550	3.2
(b) AN-$(PEO)_{20}LiClO_4$	2.9	200	2.9
(c) SDS-AN saturated solution	3.5	200	2.9
(d) SDS-AN-PEO	3.0	300	2.9

electrodes from solutions containing PEO. This procedure promotes the inclusion of the polymer electrolyte into the electrodeposited film during the formation of the composite polymer electrode. Many authors have reported that this type of composite electrode shows an improved electrochemical response in polymer-based cells of various types. In the particular case of PEO-based solid-state cells, Skotheim [9] has demonstrated the feasibility of the electrosynthesis of composite electrodes, and Watanabe and coworkers [10] have confirmed that pPy electrodes, electrosynthesized in situ from PEO electrolyte, show enhanced electrochemical behaviour.

The beneficial effect exerted by the PEO inclusion in the pPy electrodes has been further confirmed in this work. In fact, the cyclic voltammograms of samples of type (b), synthesized from a PEO-containing medium (see Table 1), show better defined oxidation and reduction waves, a smaller peak separation and a more satisfactory doping level than those related to pure pPy samples (compare figures 1a and 1b and data of Table 2).

The voltammogram of Fig. 1b also reveals a large nonfaradaic current at the end of the anodic cycle, an effect which may be described as a limiting capacitance typically associated with the redox process of polymer electrodes in general, and of polypyrrole in particular [11–13]. The origin of such capacitance can be explained on the basis of charge saturation limits and be tentatively associated with the formation of double-layer of static charge in the highly porous, thin film polymer electrode [12].

Therefore since both faradaic and capacitive currents are involved [12], the mechanism of the polypyrrole redox reaction and that of heterocyclic polymers in general, appears to be more complicated than that which only assumes that the anion (e.g. ClO_4^-) enters the polymer for charge compensation during oxidation and then leaves the polymer during the (opposite) reduction process. Indeed, there is experimental evidence that anions are not the sole difusion species in the polymer film electrode, but that cations also enter the polymer film as the anions leave [14]. Such a multiple-ion process is also feasible in the solid-state cells used in this work since anions (ClO_4^-) and cations (Li^+) are mobile in the $(PEO)_{20}LiClO_4$ polymer electrolyte [15].

On the basis of ion size, cation diffusion is expected to be faster than anion diffusion and thus the enhancement of cation transport should improve the electroactivity of the polymer electrode. The cation transport may be favoured by properly selecting the conditions of the electrosynthesis with particular attention to the nature of the doping counterion. In fact, it has been reported that by electrodeposition in the presence of large, amphiphilic surfactant ions, polypyrrole film electrodes having improved mechanical properties combined with enhanced electroactivity [16–18] can be obtained. In particular, it has been shown by various authors [17, 19, 20] and also confirmed in our laboratory [21], that pPy film electrodes synthesized in solutions containing sodium dedecyl sulphate (SDS), show fast electrochemical kinetics. This is explained by the fact that the large DS surfactant anion, incorporated into the pPy film during the electrodeposition, is not easily released in the following redox process. This situation favours the diffusion of cations for charge compensation during polymer oxidation and reduction, thus finally enhancing the kinetics of the overall redox process. Furthermore, DS ions, via a nucleophic attack, may also act as a stabilizing agent for the intermediate radical cations of the polymer, thus reducing termination processes and favouring regular chain propagations to finally promote a regular growth of the pPy film.

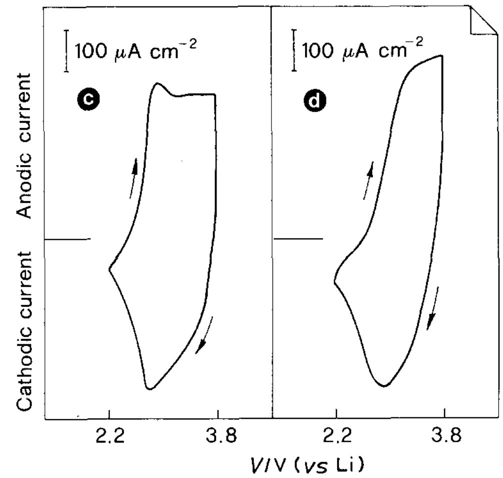

Fig. 2. Cyclic voltammetry of polypyrrole in a lithium cell having a $(PEO)_{20}LiClO_4$ polymer electrolyte. The curves are related to samples (c) and (d) and are obtained at 70°C and at $50\,mV\,s^{-1}$. For identification of samples see Table 1.

All these factors suggest that the use of pPy/DS electrodes may substantially improve the kinetics of solid-state polymer cells. This is confirmed by Fig. 2c which shows the cyclic voltammogram of a pPy/DS, sample (c) (see Table 1 for identification of the synthesis conditions). We notice from Table 2 that the voltammetric parameters are indeed enhanced. The peak separation is comparable but the cyclable charge (i.e. the doping level y) is higher than that obtained with standard pPy film electrodes (compare voltammetric data for samples (a) and (b) in the same Table 2).

Finally, appreciable response is also obtained by incorporating PEO during the electrosynthesis (see the cyclic voltammogram of Fig. 2d, related to sample (d) (Table 1 for identification).

3.2. *Impedance spectroscopy*

The interfacial and kinetic properties of the solid-state polymer electrolyte cells using pPy film electrodes, have been further examined by frequency response analysis (FRA). Indeed, this technique has been proved to be very valuable in defining the kinetic behaviour of electrochemical reactions in general [22]

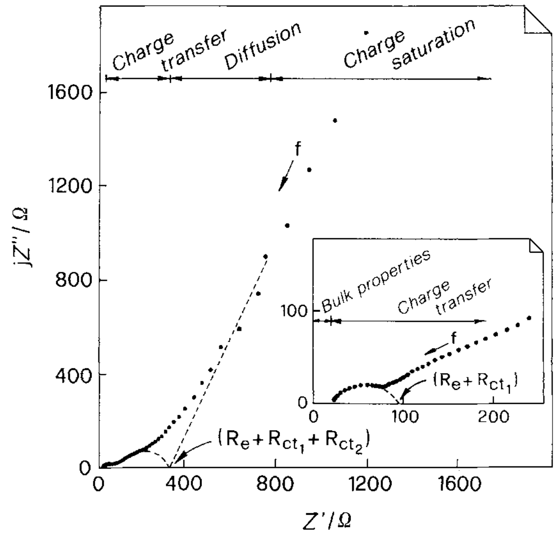

Fig. 3. Complex impedance plot at 80°C for the cell Li|$(PEO)_{20}$ $LiClO_4$|pPy (sample c). Frequency range 0.01 Hz to 100 kHz. The inset enlarges the high-frequency region.

and of the redox processes of heterocyclic polymer electrodes in particular [11–13].

Figure 3 illustrates the complex impedance plot for the cell under study, (see Scheme 1) extended over a wide frequency range. The response may be interpreted on the basis of a modified Randles circuit and of a related analysis, as described in detail in previous work [11, 24]. According to this analysis, the high frequency region refers to the bulk properties of the electrolyte and the intercept with the real axis provides the value of the electrolyte resistance R_e. In the medium-high frequency region (enlarged in the inset of Fig. 3) the impedance response is associated with the charge-transfer processes and the related relaxation effects are displayed in the diagram as semicircles whose time constants is given by the product of the interfacial charge transfer resistance R_{ct} and the double layer capacitance, C_{dl}. The value of R_{ct} can be obtained from the intercept with the real axis and that of C_{dl} from the maximum of the semicircle. In the low-frequency region the impedance response becomes representative of mass transfer, assuming a linear behaviour with a frequency-independent phase angle of $\pi/4$, represened in the equivalent circuit by the Warburg impedance Z_w. Finally, at extreme low frequencies the impedance approaches a purely capacitive response to account for limiting charge saturation effects.

Of particular interest in this investigation is the charge transfer region, from which information on the kinetics of the polymer electrode processes can be derived. However, Fig. 3 reports the impedance response of the entire cell in Expression 1, this comprising both the negative and the positive electrode interfaces. To separate the effects of the two interfaces, we have considered a symmetrical lithium cell of the type

$$\mathrm{Li}|(\mathrm{PEO})_{20}\mathrm{LiClO_4}|\mathrm{Li} \qquad (2)$$

From Fig. 4, which illustrates the complex impedance plot of this cell, two semicircles are identified. On the basis of detailed impedance analyses of the lithium/polymer electrolyte interface, discussed by us [25, 26] and other authors [27], the semicircle at higher frequencies may be associated with the charge transfer reaction

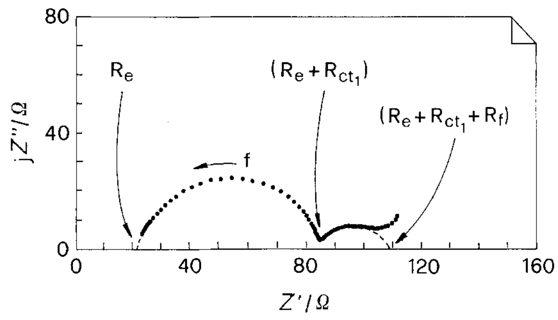

Fig. 4. Complex impedance plot at 80°C for the cell Li|$(PEO)_{20}$ $LiClO_4$|Li. Frequency range 0.01 Hz to 100 kHz. The frequencies at the masima of semicircles are 7 kHz and 1 Hz, respectively.

$$\mathrm{Li} \Longleftrightarrow \mathrm{Li}^+ + e^- \qquad (3)$$

In fact, from the frequency at the maximum of the semicircle, 7 kHz, the capacitance has been estimated to be $40\,\mu\mathrm{F\,cm^{-2}}$, i.e. a value typical of double-layer capacitance. Futhermore it is important to notice that the high-frequency semicircle develops as a complete arc which closes on the real axis, thus indicating that this interface is characterized by kinetics which approach those of an idealized charge-transfer controlled process. The intercept – which may be evaluated by a fitting program [8] – gives 60 Ω as the value of the charge-transfer resistance of the lithium interface, indicated as R_{ct1} in Fig. 4.

The second, low-frequency semicircle may be associated with a high resistive passivation film on the lithium electrode surface. Indeed, passivation phenomena, due to reaction with the elecrolyte media, are typical of the lithium interface [28]. Also the assignment of this semicircle is supported by the value of the top frequency, 1 Hz, which gives a capacitance of $6.7\,\mathrm{mF\,cm^{-2}}$, typical of thin passivation layers. The fitted intercept with the real axis gives a value of $R_{ct2} = 27\,\Omega$ as the resistance of this layer.

The characteristics of the other interface, namely of the polymer electrode/polymeric electrolyte interface were analysed by frequency response analysis of symmetrical cells of the type

$$\mathrm{pPy}|(\mathrm{PEO})_{20}\mathrm{LiClO_4}|\mathrm{pPy} \qquad (4)$$

using, in turn couples of pPy electrode samples prepared with the four different conditions illustrated in Table 1. It is important to point out that each selected couple of pPy electrode samples was deposited from the same solution and under the same conditions, in order to avoid asymmetry effects in the testing cell. Furthermore, to assure an effective comparison between the various samples, the same thickness was used for each selected polymer film electrode couple.

The related frequency response confirms that the conditions of synthesis of the electrodes are crucial in determining the morphology of the interfaces of the solid-state cell and thus the kinetics of the electro-

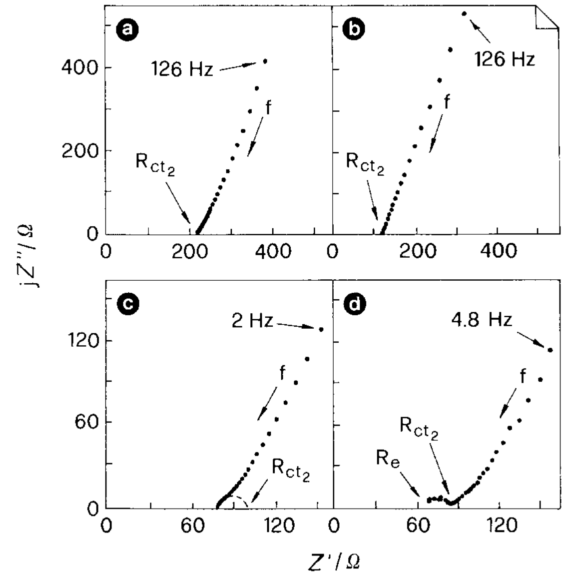

Fig. 5. Complex impedance plot at 80°C for the cell pPy|$(PEO)_{20}LiClO_4$|pPy. The four plots are related to couples of pPy samples of types (a), (b), (c) and (d), respectively. For identification of samples see Table 1. All the plots are extended to 65 kHz.

chemical process. Indeed, Fig. 5a, which illustrates the response of a cell using pPy samples of type (a), only reveals the Warburg-type diffusion line, without any evidence of a charge-transfer semicircle. This clearly indicates that in this case the electrochemical process is entirely diffusion-controlled. Furthermore, the interfacial resistance, evaluated by the intercept to the real axis (R_{ct2} in Fig. 5) is very high, as expected on the basis of the poor electrode-to-electrolyte contact conditions.

Also in cells using pPy-PEO composite samples, the response indicate mere diffusion-controlled kinetics (Fig. 5b). However, the conditions of the interface are consistently improved, as indicated by the lower value of R_{ct2}.

When using pPy/DS samples, a part of the charge-transfer semicircle becomes apparent (Fig. 5c), this in agreement with the fact the presence of the large surfactant anion favours faster kinetics and more regular growth of the pPy chains. Finally, the use of pPy/SDS–PEO composite electrodes gives an impedance response characterized by an almost complete semicircular arc (Fig. 5d), this confirming that this type of electrode is the most favourable in assuring the fastest kinetics and the lowest interfacial resistance (notice the value of R_{ct2} in Fig. 5d) in solid-state polymer cells of the type examined in this work.

4. Conclusions

The voltammetric and complex impedance results indicate that the morphology of the interfaces plays a key role in the electrochemical performances of solid-state cells based on the combination of polymer electrolytes and polymer electrodes. The development of these cells for practical application will require full optimization of the interfacial contact conditions. Following the evidence discussed in this work, various approaches may be considered to achieve this goal:

(a) electrodeposition of the pPy electrodes directly from a PEO-based solution;

(b) formation of composite pPy films with optimized composition ratio between polymer electrode, surfactant anion and polymer electrolyte;

(c) improvement in the electrode flexibility by inclusion of plasticizers in the composite mixtures.

Those approaches are presently under test in our laboratory and their impact on the electrochemical behaviour of the solid-state polymer cells will be discussed in following papers.

Acknowledgements

This work was carried out with the financial support of the Consiglio Nazionale delle Ricerche, Progetto Finalizzato Energetica 2 (Contract CNR No. 88.01359.59) and of the Commission of the European Community (Contract no. EN3E/145/I), within the EC Non-Nuclear Energy Programma).

References

[1] B. Scrosati, *Prog. Solid State Chem.* **18** (1988) 1.
[2] R. Linford (Ed.), 'Electrochemical Science and Technology of Polymers', Elsevier Applied Science, London (1987).
[3] S. Panero, P. Prosperi and B. Scrosati, *Electrochim. Acta* **32** (1987) 1461.
[4] F. Croce, S. Panero, P. Prosperi and B. Scrosati, *Solid State Ionics* **28–30** (1988) 895.
[5] P. Novak, I. Inganas and R. Bjorklund, *J. Electrochem. Soc.* **134** (1988) 1341.
[6] P. Novak and I. Inganas, *ibid.* **135** (1988) 2485.
[7] C. Arbizzani and M. Mastragostino, *Electrochim. Acta* **35** (1990) 251.
[8] B. A. Boukamp, *Solid State Ionics* **20** (1986) 31.
[9] T. A. Skotheim, *Synth. Met.* **14** (1986) 31.
[10 M. Watanabe, K. Tadano, K. Sanui and N. Ogata, *Chemistry Letters* (1989) 1239.
[11] S. Panero, P. Prosperi, S. Passerini, B. Scrosati and D. D. Perlmutter, *J. Electrochem. Soc.* **136** (1989) 3729.
[12] N. Marmillod, J. Tanguy and F. Petiot, *ibid.* **133** (1986) 1073.
[13] J. Tanguy, N. Marmillod and M. Hoclet, *ibid.* **134** (1987) 795.
[14] J. H. Kaufman, K. K. Kanazawa and G. B. Street, *Phys. Rev. Lett.* **53** no. 26, (1984) 2641.
[15] J. R. MacCallum and C. A. Vincent (Eds), 'Polymer Electrolyte Review I', Elsevier Applied Science, London (1987).
[16] M. Gatoh, K. Kaneto and K. Yoshino, *Synt. Met.* **14** (1986) 289.
[17] W. Wernet, M. Monkenbusch and G. Wegner, *Makround Chem. Rapid commun.* **5** (1984) 157.
[18] L. F. Waren and D. P. Anderson, *J. Electrochem. Soc.* **134** (1987) 105.
[19] R. C. D. Peres, J. M. Pernaut and M. A. De Paoli, *Synth. Met.* **27** (1989) C59.
[20] J. M. Pernaut, R. C. D. Peres, V. F. Juliano and M. A. De Paoli, *J. Electroanal. Chem.* **274** (1989) 225.
[21] M. A. De Paoli, S. Panero, P. Prosperi and B. Scrosati, *Electrochim. Acta*, submitted.
[22] J. R. Macdonald, 'Impedance Spectroscopy', John Wiley, London (1987).
[23] T. B. Hunter, P. S. Tyler, W. H. Smyrl and H. S. White, *J. Electrochem. Soc.* **134** (1987) 2198.
[24] S. Panero, P. Prosperi, D. Zane and B. Scrosati, *J. Appl. Electrochem.*, submitted.
[25] B. Scrosati, *Br. Polym. J.* **20** (1988) 219.
[26] Idem, *J. Electrochem. Soc.* **136** (1989) 2774.
[27] D. Fauteux, *Solid State Ionics* **17** (1985) 133.
[28] B. Scrosati, in 'Polymer Electrolyte Reviews I, (edited by J. MacCallum and C. A. Vincent) Elsevier Applied Science, London (1987) p. 315.